06

AFM study of the morphology of elastomers based on polyurethanimides with various rigid and flexible fragments

© T.E. Sukhanova,[1] V.M. Svetlichniy,[2] D.A. Kuznetsov,[2] M.E. Vylegzhanina,[2] G.V. Vaganov,[2] N.V. Lebedev[1]

[1] Lebedev Institute of Synthetic Rubber,
198035 St. Petersburg, Russia
[2] Institute of Macromolecular Compounds, Russian Academy of Sciences,
199004 St. Petersburg, Russia
e-mail: tat_sukhanova@bk.ru, valsvet@hq.macro.ru

The morphological characteristics of the surface of a number of films of elastomers based on polyurethanimides (PUI) were studied by atomic force microscopy (AFM). Significant differences in the surface morphology of PUI films were found depending on the composition: from granular morphology with different grain sizes or spongy morphology with nano - and submicron pores and cavities on the surface, to spherulitic morphology. It is shown that the roughness of the free surfaces formed during the films formation from the solution is significantly lower than the roughness of the surface which was in contact with the substrate. The influence of the chemical structure and size of the rigid diamine fragments in PUI macromolecules on the morphology of the film surface and the presence of different phases in the AFM torsion mode is established. The comparison of the deformation and strength characteristics showed high values of the elongation at break (more than 1400%) in the PUI films with a developed porous structure of both surfaces. The results obtained show the need to control and take into account the morphological parameters of the surface layers of products made of highly elastic imide-containing materials for their use for technical and other purposes.

Keywords: synthesis of polyurethanimides, atomic-force microscopy, elastomer films morphology, surface roughness, viscosity and strain-strength characteristics.

Introduction

Currently the researchers pay closer attention to the so called segmented polymers, main chains of which are made in such a way, that rigid and flexible blocks are included in each repeating unit [1–5]. Such chemical structure defines the specifics of their mechanical properties — lack of fragility and elasticity in the wide range of temperature. This approach is used at formation of thermoelastoplasts based on segmented polyurethanes [1,2] with increased elastic properties. Multiblock (segmented) copolymers, containing rigid imide blocks and flexible blocks of aliphatic ethers or esters — copolyetherimides (coPEI), or polyurethanes — copolyurethanimides (coPUI) [3,4,6], hold a special place among thermoelastoplasts. Variability of chemical composition and length of rigid and flexible blocks, as well as their interrelations in the chains influence the supramolecular structure, thermal resistance, viscoelastic and other properties of these polymers [4–6]. Works, performed in the area of synthesis and research of thermoelastoplasts properties, are of interest to modern science and technologies, that are in desperate need of thermal resistant and high heat resistant elastic polymer materials.

Earlier, based on multiblock coPUI and coPEI matrices, we developed and characterized in detail the wide range of elastomers, capable to operate under extreme conditions, including high temperatures and pressure drops. We obtained nanocomposites based on them, containing nanofillers of various type: carbon nanoparticles of various geometry, structures and morphologies (single-wall carbon nanotubes and nanofibres, graphene), nanoparticles of zirconium dioxide (ZrO_2), tungsten disulfide and diselenide (WS_2 and WSe_2), and we also synthesized and researched compositions based on coPEI, modified with silicone resin (MQ-resin). Fillers content was changed in a wide range of concentrations (from 0.1 to 10 wt.%). The performed researches showed that chemical structure of synthesized coPUI and coPEI, sizes and interrelation of rigid and flexible fragments in macromolecules, composition, structure and morphology of introduced nanoparticles of metal chalcogenides or MQ-resin, their concentration in composite, as well as nature of substrate (glass, fluoroplastic, aluminum foil or polyimide film), onto which the coPUI or coPEI composite films were poured, significantly influence structural-morphological, physico-mechanical, tribological and other characteristics of produced nanomaterials [7-12].

№ 1

№ 2

№ 3
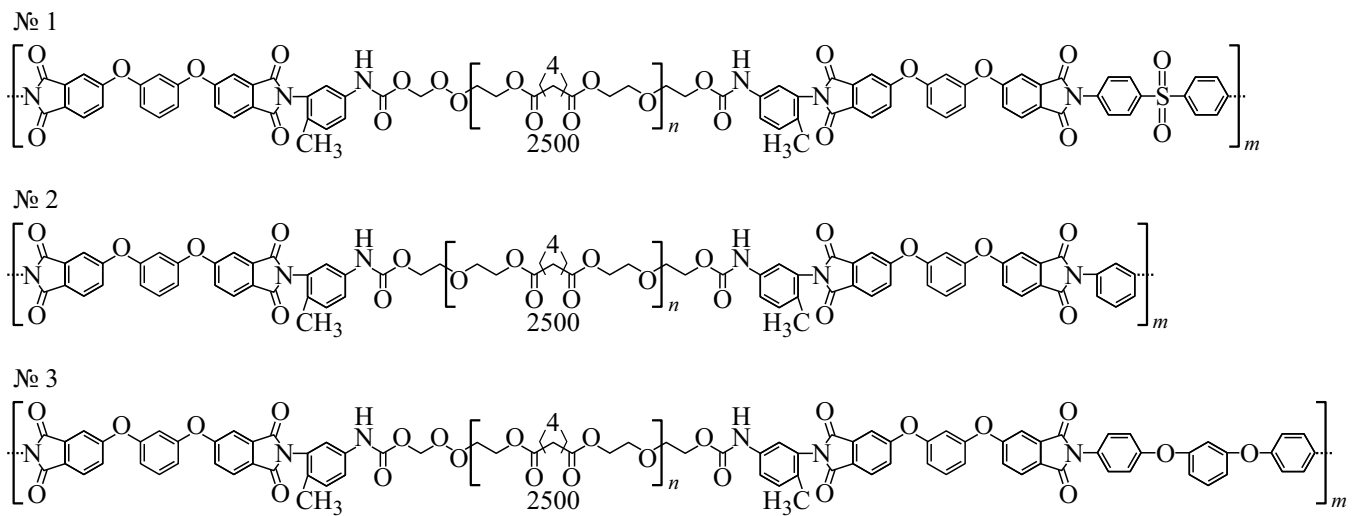
Figure 1. Structure formulas of synthesized PUI.

Table 1. AFM torsion mode images of upper and lower surface of PUI samples, values of their roughness and inherent viscosity of solutions $[\eta]$, from which the films were poured

№ 1 2500-TDI-R-Dapsone	№ 2 2500-TDI-R-mF	№ 3 2500-TDI-R-RD
top, scan matrix size — $12 \times 12\,\mu$m		
bottom, scan matrix size — $12 \times 12\,\mu$m		
$[\eta] = 0.48$	$[\eta] = 0.93$	$[\eta] = 0.99$
$R_a = 2.1\,$nm $R_q = 2.9\,$nm	$R_a = 1.5\,$nm $R_q = 1.9\,$nm	$R_a = 1.2\,$nm $R_q = 1.5\,$nm
$R_a = 20.3\,$nm $R_q = 26.8\,$nm	$R_a = 10.5\,$nm $R_q = 13.0\,$nm	$R_a = 35.1\,$nm $R_q = 44.0\,$nm
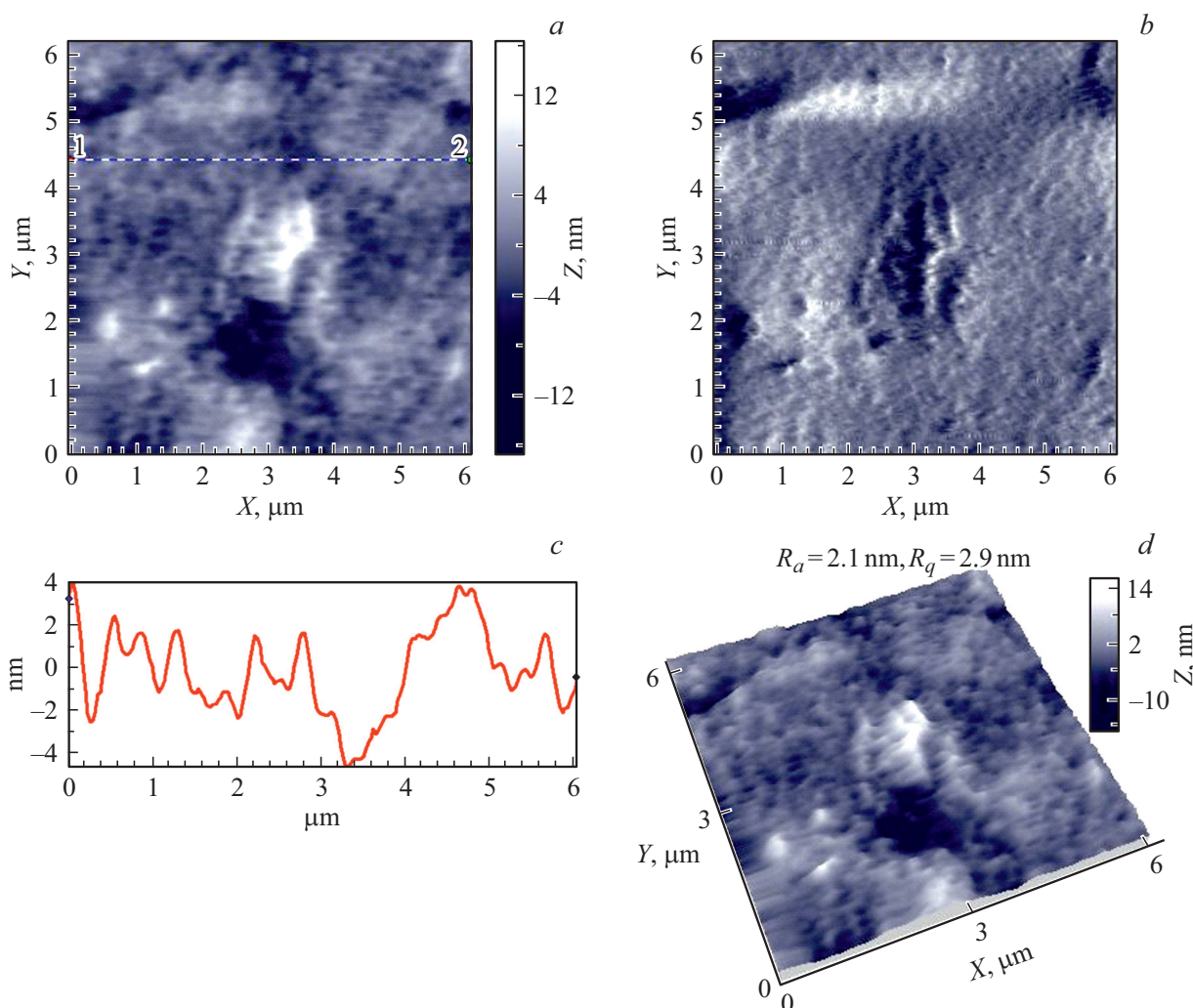
Figure 2. AFM images of the surface of the film 2500-TDI-R-Dapsone (sample № 1), free surface; a — topography, b — lateral forces contrast, c — profile of the selected surface area, d — 3D image.

The purpose of this study was synthesis and research of morphology of a surface of polyurethanimides-based elastomer films on nano- and micro-levels using atomic force microscopy (AFM) method, determination of correlation of their structural-morphological characteristics with physico-mechanical properties.

1. Experimental part

PUI synthesis was performed as per [13]. By means of example of sample № 1 (2500-TDI-R-Dapsone): synthesis was performed in a three-neck flask equipped with entry for argon and mechanical mixer. 2.5 g (1 mmol) of polydiethyleneglycoladipate ($M_n = 2.5 \cdot 10^3$) and 0.348 g (2 mmol) of 2,4-toluene diisocyanate were loaded into the flask. This mixture was mixed at 80°C for 1 h, and then 0.804 g (2 mmol) of dianhydride R (4, 4′-(1,3-phenylenebis(oxy))bis(phthalic anhydride) was added and mixed at 180°C for 2 h. The resulting melt was dissolved in

8 ml of N,N-dimethylacetamide (DMAA) and the solution was cooled until room temperature. Then to the resulting solution of macromonomer, containing end anhydride groups, 0.248 g (1 mmol) of 4, 4′-sulphonyldianiline was added and mixed for 18 h, resulting in prepolymer forming — polyamide acid (PAA). Structure formulas of PUI № 1−№ 3, containing various rigid blocks, are presented in Fig. 1.

Effective contour length of flexible block „diol 2500" for all copolymers was the same and equal to $L \sim 22.5$ nm, contour lengths of rigid blocks were different: for sample № 1 — $L \sim 7$ nm, № 2 — ~ 6.1 nm, № 3 — ~ 7.5 nm.

Surface topography study and evaluation of mechanical characteristics were performed on polymer films, obtained under the same conditions by forming from 30% solutions of polyurethaneamic acid by pouring onto glass substrates with the following step warming as per the regime: 80°C — 16 h, 120°C — 1 h, 140°C — 1 h, 160°C — 2 h. Then the films were exposed in distilled water for 2 h, removed
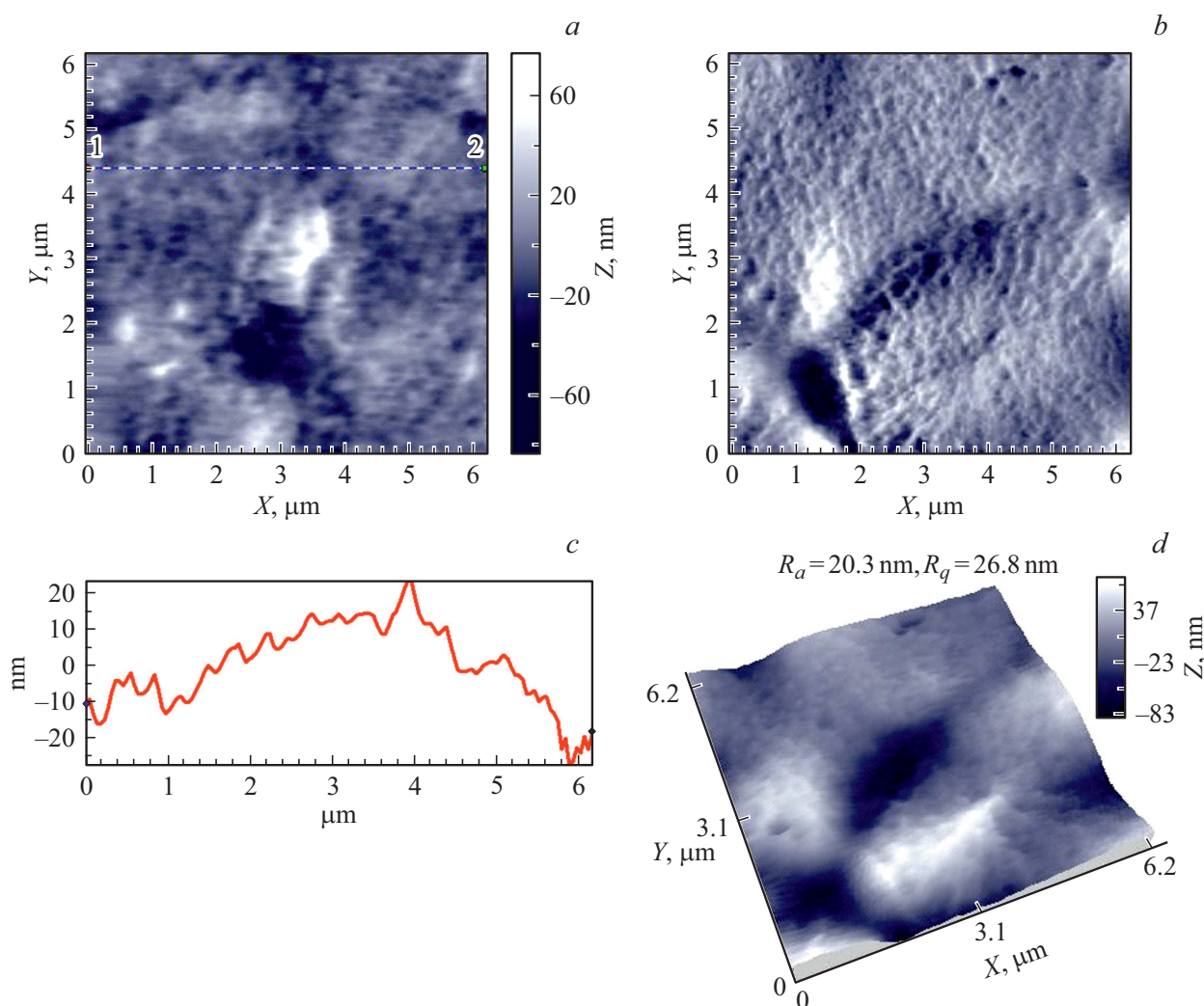
Figure 3. AFM images of the surface of the film 2500-TDI-R-Dapsone (sample № 1), surface to substrate (bottom): a — topography, b — lateral forces contrast, c — profile of the selected surface area, d — 3D image.

from substrates and dried under room temperature. After removal from the substrates the films were not warmed.

Stress-strain characteristics of PUI films were defined in uniaxial tension mode on samples in the form of strips with 2 mm width and working section length of 25 mm. Tests were performed using general-purpose testing system Instron 5940 (Instron, USA) with deformation rate of 50 mm/min. During tests the sample tensile diagram was registered (online), upon the results of the tests the elastic modulus E, rupture resistance σ_p and elongation at break ε_p were determined.

Inherent viscosity of copolymer solutions were determined using Ubbelohde viscometer. 0.5% copolymer solutions in N-methyl-2-pyrollidone (N-MP) were used for measurements.

Morphological studies of synthesized PUI films were performed using atomic force microscope Nanotop NT-206 (ODO „Mikrotestmashyny", Belarus). Measurements were performed in contact mode under atmospheric condi-

tions using silicon cantilevers NSC11/AlBS with stiffness coefficient $k = 3.0\,\text{N/m}$ and tip curve radius of 10 nm. Experimental data were processed using Surface Explorer software.

2. Results discussion

Fig. 2 shows AFM images of fragments of top (free) surface of the film 2500-TDI-R-Dapsone (sample № 1). It can be observed that this surface is sufficiently smooth, with fine-grained morphology. There are multiple irregular-shaped inclusions, formed by elongated chain aggregates. These aggregates are relatively uniformly distributed over the whole film surface, as shown in torsion mode for scan matrix $12 \times 12\,\mu\text{m}$ (Table 1). Their height above „averaged surface" level reaches value of 4 nm (Fig. 1, c). In torsion mode for scan matrix $6 \times 6\,\mu\text{m}$ (Fig. 1, b) it can be observed that these inclusions can belong to
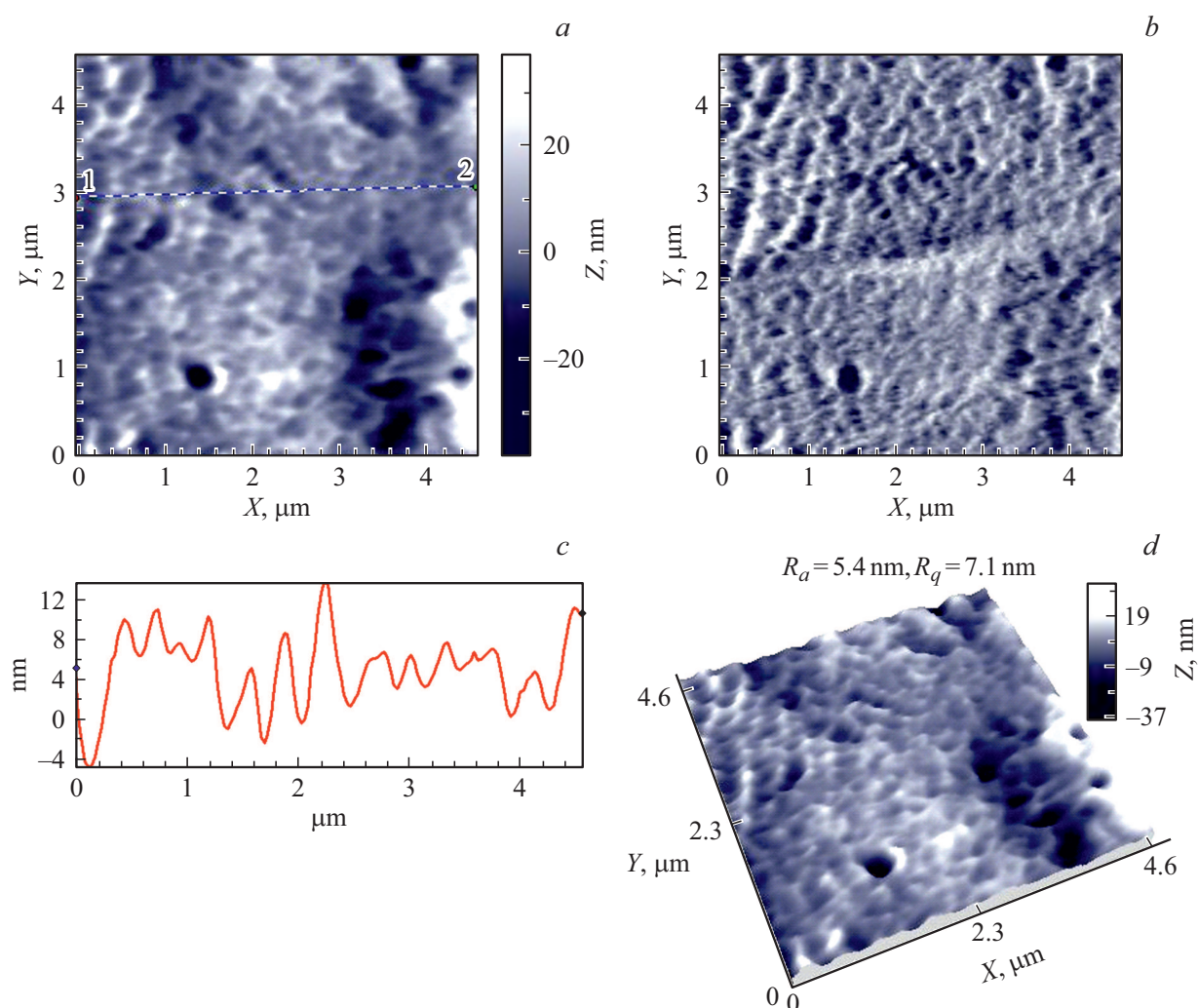
Figure 4. AFM images of the central area of spherolite, observed in the film 2500-TDI-R-Dapsone (sample № 1) on a surface to substrate (bottom); *a* — topography, *b* — lateral forces contrast, *c* — profile of the selected surface area, *d* — 3D image.

another phase, since they have different friction coefficient (differ by contrast from the base surface [14]). Values of arithmetic mean and root-mean-square roughness of the top surface of the sample № 1 for scan matrix $6 \times 6 \mu$m are $R_a = 2.1$ nm and $R_q = 2.9$ nm, respectively.

Table 1 also includes AFM images of top and bottom surfaces of the samples № 2 and № 3 in torsion mode (scan matrix size is $12 \times 12 \mu$m), values of inherent viscosity for solutions $[\eta]$, from which the films were poured, and roughness values (R_a and R_q) for top and bottom surfaces of all samples under study.

On the bottom surface of the film 2500-TDI-R-Dapsone (Fig. 3, Table 1) the spherolites, diameter of which changes from 2 to 12μm, are well visible. On AFM images of this surface (Fig. 3, *a, d*) the fragments of four contacting spherolites can be noticed; height of the central part of one of them above the level of „averaged surface" reaches 20 nm (Fig. 3, *c*). In Fig. 3, *b* in torsion mode the multiple fibrils

with thickness of at least 100 nm, of which the spherolites consist, are well visible. Values of surface roughness for scan matrix $6 \times 6 \mu$m are equal to $R_a = 20.3$ nm and $R_q = 26.8$ nm.

At higher resolution AFM images of thin structure of the spherolites central part on the bottom surface of the sample № 1 (Fig. 4, scan matrix $5 \times 5 \mu$m) the porous fibrillar morphology with fibrils with thickness of ~ 100 nm is well visible. The same fibrillar morphology is visible on AFM image of the peripheral part of spherolites in Fig. 3, *b* in torsion mode. Formed spherolites with fibrillar morphology are high-porous spherical formations with polygonal or close-to-spherical shape due to steric restrictions during their growth.

Fig. 5 shows AFM images of the fragment of top surface of the thin film 2500-TDI-R-mF (sample № 2). It can be observed that free (top) surface of the sample 2500-TDI-R-mF is smooth, with well-defined fine-grained morphology with grains size of less than 100 nm. Multiple
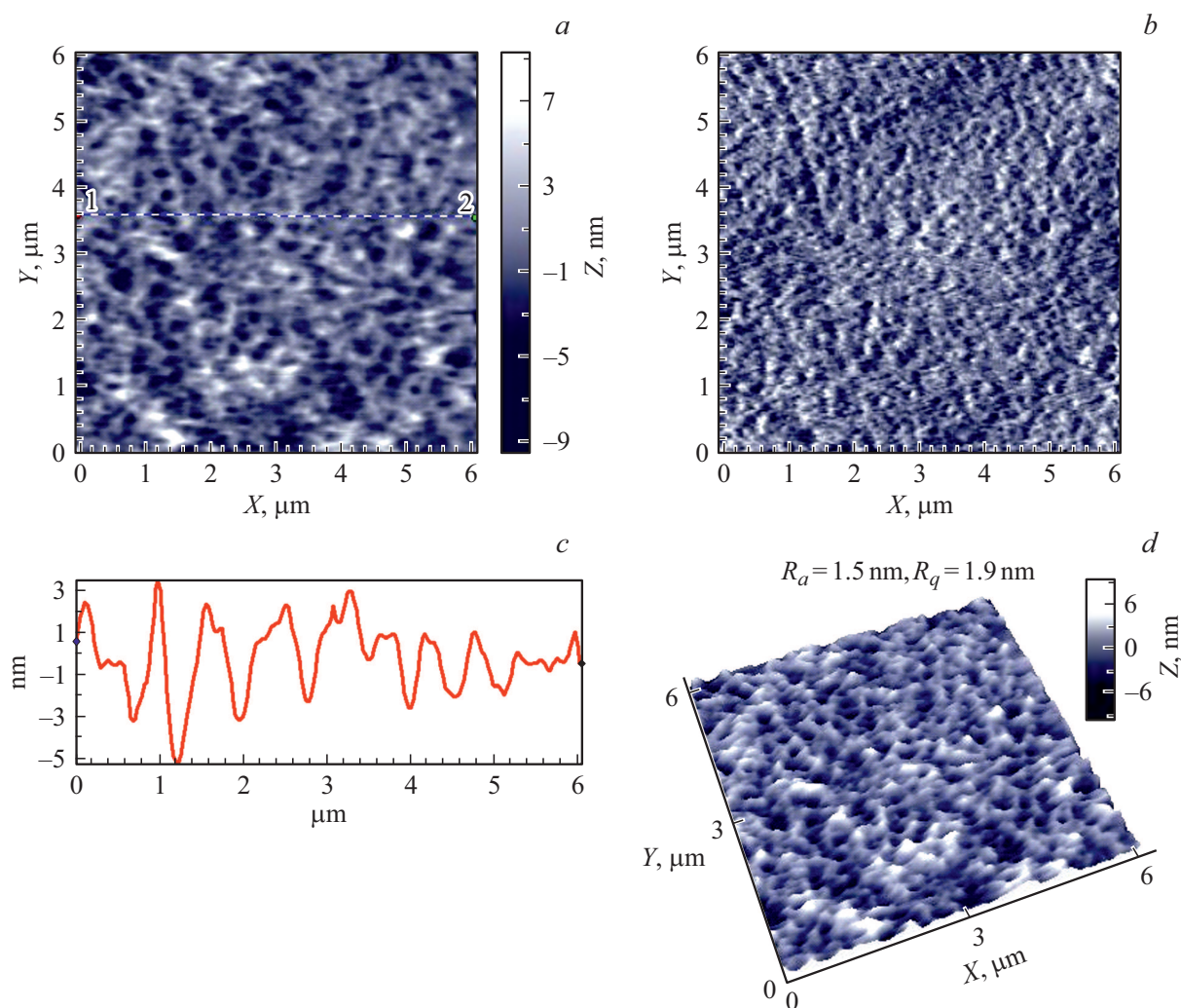
Figure 5. AFM images of the surface of the film 2500-TDI-R-mF (sample № 2), free surface; *a* — topography, *b* — lateral forces contrast, *c* — profile of the selected surface area, *d* — 3D image.

pores with diameter of $50-200$ nm, forming clusters with $5-10$ nanopores each in some places, are observed on the surface. Pores are sufficiently uniformly distributed over the whole film surface. Their height above „averaged surface" is low and reaches value of $2-3$ nm. In torsion mode (Fig. 5, *b*) and surface profile (Fig. 5, *d*) it is well visible that the surface is high-porous and nanostructured. Values of surface roughness for scan matrix $6 \times 6 \mu$m are equal to $R_a = 1.5$ nm and $R_q = 1.9$ nm. It is possible that pores were formed during the process of imidization of prepolymer — polyamide acid at DMAA solvent removal and water, coming out during imidization.

On the bottom surface (surface to substrate) of the film 2500-TDI-R-mF (Fig. 6) the pores are also well visible, but they are almost twice bigger, than on top surface, their dimensions are $100-500$ nn, while height above „averaged surface" level reaches $30-50$ nm. Values of arithmetic mean and root-mean-square roughness of the surface for scan matrix $6 \times 6 \mu$m are $R_a = 10.5$ nm and $R_q = 13.0$ nm.

Presence of such developed porosity on both surfaces of the film allows to assume that the sample is also high-porous in volume, i.e. the sample 2500-TDI-R-mF is a „foam" material with spongy morphology.

Top surface of the film 2500-TDI-RD (sample № 3) (Fig. 7) has fine-grained morphology with grains size from 50 to 200 nm. There are multiple pores with diameter of less than 200 nm on the surface. Pores are sufficiently uniformly distributed over the whole film surface. Their height above „averaged surface" reaches value of 5 nm. In torsion mode (Fig. 7, *b*) the elongated fibrillar formations can be noticed. In some areas of film surface these fibrils are oriented in orthogonally related directions, suggesting on high level of nanostructurization of the sample surface. Values of surface roughness for scan matrix $6 \times 6 \mu$m are equal to $R_a = 1.2$ nm and $R_q = 1.5$ nm, respectively.

On the bottom surface of the film 2500-TDI-R-RD (Fig. 8) the irregular-shaped cavities and craters of
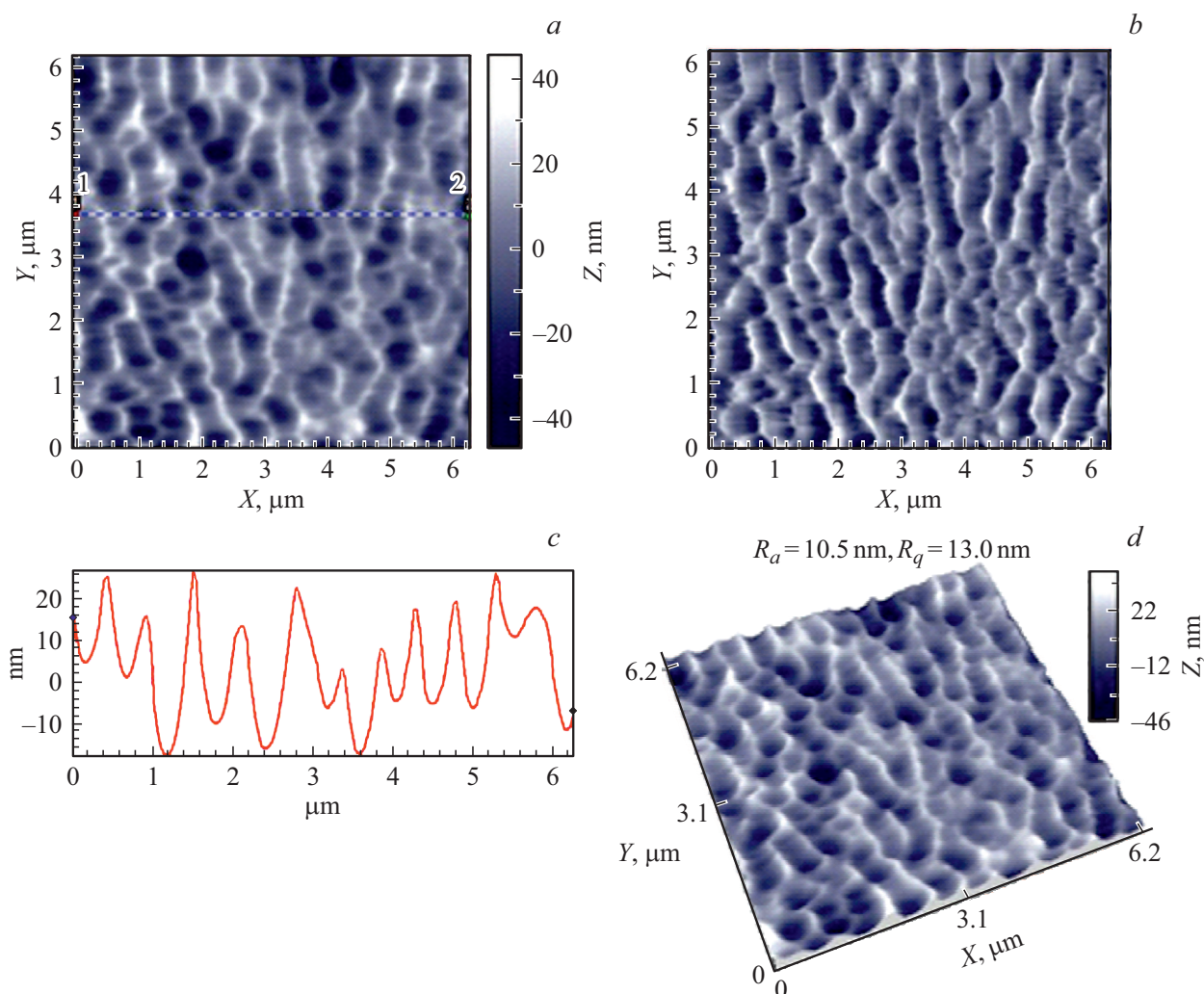
Figure 6. AFM images of the surface of the film 2500-TDI-R-mF (sample № 2), surface to substrate (bottom): a — topography, b — lateral forces contrast, c — profile of the selected surface area, d — 3D image.

submicron-size with a depth of about 200 nm are well visible. Presence of such craters on the bottom surface of the sample results in high values of arithmetic mean and root-mean-square roughness of the surface — for scan matrix $8 \times 8\,\mu$m they are equal to $R_a = 35.1$ nm and $R_q = 44.0$ nm.

Analysis of the results, presented in Table 1, shows that all samples are characterized by very smooth top (free) surface — values of arithmetic mean roughness are $R_a = 1.2-2.1$ nm regardless of values of inherent viscosity of initial solutions. Sample № 1 (2500-TDI-R-Dapsone) has the lowest value of inherent viscosity $[\eta] = 0.48$, and that, apparently, causes spherolites formation in a volume of polymer film, adjacent to substrate. Hydrophobic interactions and poor wetting of glass substrate with polymer solutions are also influence on spherolites forming.

Comparison of inherent viscosity of synthesized sample solutions showed that sample № 3 (2500-TDI-R-RD) has the biggest value of inherent viscosity of $[\eta] = 0.99$ among

polymers under study, while also having the most developed nanostructured porous morphology on films free surface and large pores on bottom surface. Sample № 2 with closer value of $[\eta] = 0.93$ has the same morphology type, but finer and more regular porosity on both surfaces of the film. By contrast, the value of inherent viscosity for sample № 1 is two times lower ($[\eta] = 0.48$) than samples № 2 and № 3. Since it is known, that value of inherent viscosity is related to polymer molecular mass (MM), it can be said that MM of samples № 2 and № 3 is significantly higher than of sample № 1, that certainly influences the mechanical characteristics of films.

Table 2 includes stress-strain characteristics of PUI films. It is interesting that samples № 1 and № 2 have close values of elastic modulus, but rupture resistance and elongation at break of sample № 1 are significantly lower than of samples № 2 and № 3. At the same time, sample № 3 has values of rupture resistance and elongation at break that are close to sample № 2, but elastic modulus of
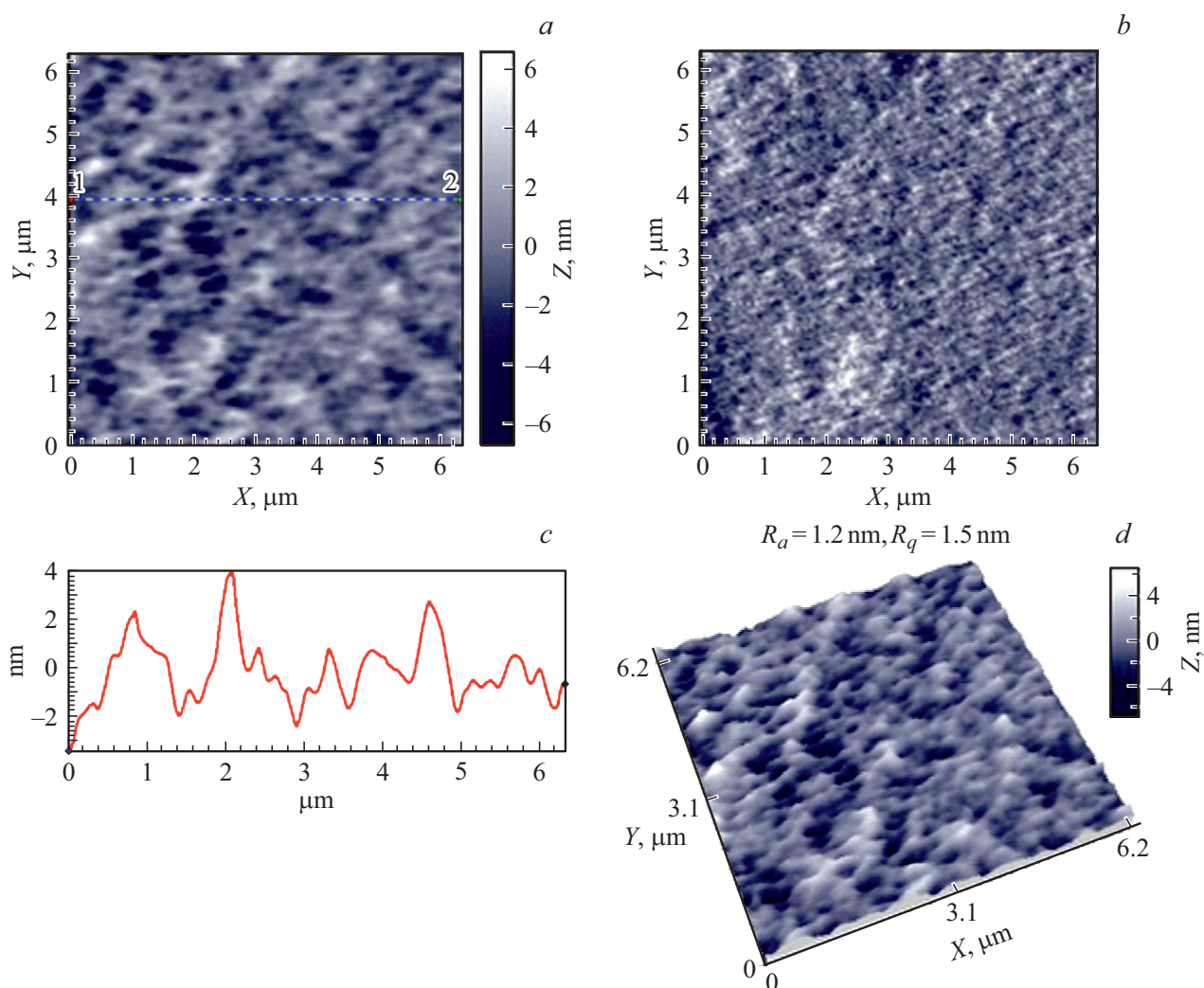
Figure 7. AFM images of the surface of the film 2500-TDI-R-RD (sample № 3), free surface; *a* — topography, *b* — lateral forces contrast, *c* — profile of the selected surface area, *d* — 3D image.

Table 2. Stress-strain characteristics of PUI, containing various rigid and flexible fragment

PUI	E, MPa	σ_p, MPa	ε_p, %
№ 1	6.1 ± 0.5	10.4 ± 0.1	995 ± 19
№ 2	6.2 ± 0.4	42.9 ± 4.9	1431 ± 82
№ 3	4.9 ± 0.6	44.5 ± 1.9	1433 ± 28

this polymer is significantly lower. That means that the sample with spherulitic morphology is significantly inferior to nanostructured and more uniform surface-porous samples in terms of strength and elasticity. Such differences in mechanical characteristics of studied samples can be explained by the difference in morphology and different values of MM. On X-ray level all samples were amorphous.

Conclusion

The morphology of the surfaces of synthesized PUI films, containing flexible block and rigid blocks of various length and molecular structure, was studied by AFM method; roughness parameters of both surfaces of PUI films were defined. It was shown that synthesized PUI samples have various morphology nature, various supramolecular structure and porosity of near-surface layers of films.

Observed results of mechanical tests showed that synthesized PUI films are sufficiently strong and high-elastic (elongation at break reaches 1433%). Due to multiblock morphology, characteristic for these polymers, the synthesized PUI are promising materials for processing from melt and obtaining the elastic sizable casted products — moldings [13].
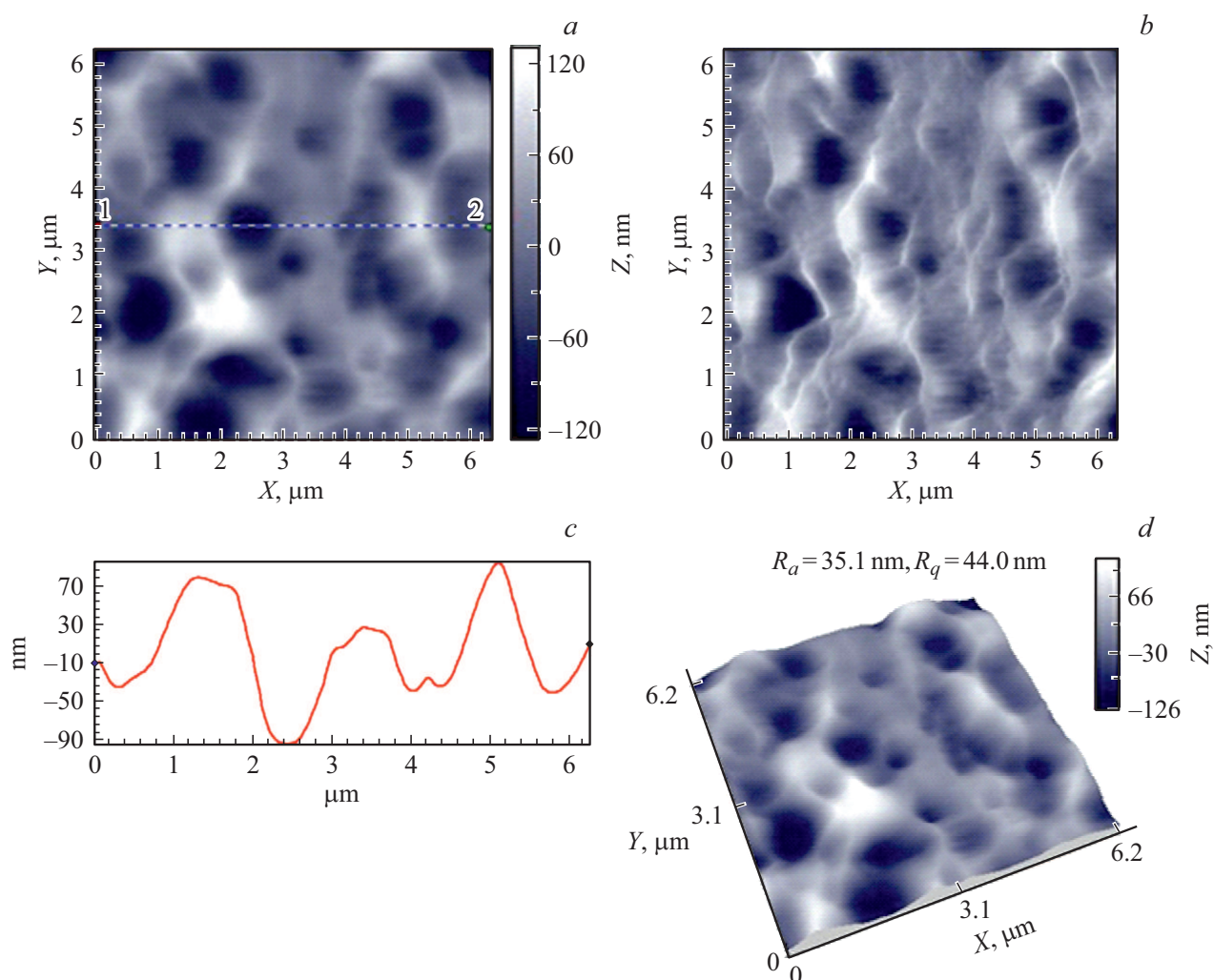
Figure 8. AFM images of the surface of the film 2500-TDI-R-RD (sample № 3), surface to substrate (bottom): *a* — topography, *b* — lateral forces contrast, *c* — profile of the selected surface area, *d* — 3D image.

Funding

Conflict of interest

The authors declare that they have no conflict of interest.

References

[1] I. Yilgor, E. Yilgor, G.L. Wilkes. Polymer, **58**, A1 (2015). https://doi.org/10.1016/j.polymer.2014.12.014

[2] B. Finnigan, K. Jack, K. Campbell, P. Halley, R. Truss, Ph. Casey, D. Cookson, S. King, D. Martin. Macromolecules, **38**, 7386 (2005). https://doi.org/10.1021/ma0508911

[3] J. Chena, J. Zhanga, T. Zhua, Z. Huaa, Q. Chenb, X. Yub. Polymer, **42**, 1493 (2001). DOI: 10.1016/S0032-3861(00)00527-9

[4] T. Kogiso, S. Inoue. J. Appl. Polymer. Sci., **115**, 242 (2010). https://doi.org/10.1002/app.31126

[5] R.J. Gaymans. Prog. Polym. Sci., **36** (6), 713 (2011). DOI: 10.1016/j.progpolymsci.2010.07.012

[6] V.E. Yudin, V.E. Smirnova, A.L. Didenko, E.N. Popova, I.V. Gofman, A.V. Zarbuev, V.M. Svetlichnyi, V.V. Kudryavt-sev. Russ. J. Appl. Chem., **86** (6), 920 (2013). DOI: 10.1134/S1070427213060232

[7] T.E. Sukhanova, T.A. Kuznetsova, V.A. Lapitskaya, T.I. Zubar, S.A. Chizhik, M.E. Vylegzhanina, A.A. Kutin, A.L. Didenko, V.M. Svetlichnyi. *Atomic-Force Microscopy and Its Applications*. Ed. by T. Tański, M. Staszuk, B. Ziębowicz (IntechOpen, London, 2019), p. 69. DOI: 10.5772/intechopen.78625

[8] T.A. Kuznetsova, T.I. Zubar, V.A. Lapitskaya, K.A. Sudzilouskaya, S.A. Chizhik, A.L. Didenko, V.M. Svetlichnyi, M.E. Vylegzhanina, V.V. Kudryavtsev, T.E. Sukhanova. IOP Conf. Ser.-Mat. Sci., **256**, 012022 (2017). DOI: 10.1088/1757-899X/256/1/012022

[9] T.E. Sukhanova, T.A. Kuznetsova, M.E. Vylegzhanina, V.M. Svetlichnyi, A.A. Kutin, T.I. Shiryaeva, S.A. Chizhik. Tez. dokl XIX Mezhd. simp. *„Nanofizika i nanoelektronika"* (N. Novgorod, Rossiya, 2015), t. 1, s. 292–295 (in Russian).

[10] T.E. Sukhanova, T.A. Kuznetsova, M.E. Vylegzhanina, A.L. Didenko, D.A. Kuznetsov, V.M. Svetlichnyi, T.I. Zubar, V.A. Lapitskaya, K.A. Sudilovskaya, A.Ya. Volkov, A.A. Kutin, V.V. Kudryavtsev, S.A. Chizhik. Nanotekhnologii: nauka i proizvodstvo, **4**, 55 (2017) (in Russian).

[11] T.E. Sukhanova, T.A. Kuznetsova, M.E. Vylegzhanina, V.M. Svetlichnyi, T.I. Zubar, S.A. Chizhik. Sb. dokl. XII Mezhd. konf. *„Metodologicheskie aspekty skaniruyushchey zondovoy mikroskopii BelSZM-2016"* (Minsk, Belarus, 2016), s. 8–17 (in Russian).

[12] T.E. Sukhanova, T.A. Kuznetsova, M.E. Vylegzhanina, V.A. Lapickaya, A.A. Kutin, A.L. Didenko, V.M. Svetlichnyi, S.A. Chizhik. *Sb. dokl. XXIV Mezhdunarodnogo simpoziuma „Nanofizika i nanoelektronika"* (N. Novgorod, Rossiya, 2020), t. 1, s. 400–401 (in Russian).

[13] D.A. Kuznetsov, V.M. Svetlichnyi, A.L. Didenko, G.V. Vaganov, V.Yu. Elokhovsky, V.V. Kudryavtsev, V.E. Yudin. ZhPH, **93** (10), 1418 (2020). DOI: 10.31857/S0044461820100023

[14] V.L. Mironov. *Osnovy skaniruyushchey zondovoy mikroskopii* (Institut fiziki mikrostruktur RAN, N. Novgorod, 2004) (in Russian).